

Article

β -Carotene from the Alga *Dunaliella bardawil* Decreases Gene Expression of Adipose Tissue Macrophage Recruitment Markers and Plasma Lipid Concentrations in Mice Fed a High-Fat Diet

Nir Melnikov^{1,2,†}, Yehuda Kamari^{1,2}, Michal Kandel-Kfir¹, Iris Barshack^{1,2}, Ami Ben-Amotz³, Dror Harats^{1,2}, Aviv Shaish^{1,4,†} and Ayelet Harari^{1,*,†}

¹ The Bert W. Strassburger Metabolic Center, Sheba Medical Center, Ramat Gan 5262000, Israel; nir.melnikov@sheba.gov.il (N.M.); yehuda.kamari@sheba.gov.il (Y.K.); michal.kandel.kfir@sheba.gov.il (M.K.-K.); iris.barshack@sheba.gov.il (I.B.); dror.harats@sheba.gov.il (D.H.); aviv.shaish@sheba.gov.il (A.S.)

² The Sackler Faculty of Medicine, Tel-Aviv University, Tel-Aviv 6997801, Israel

³ N.B.T., Nature Beta Technologies Ltd., Eilat 8851100, Israel; amiba@bezequin.net

⁴ The Department of Life Sciences, Achva Academic College, Arugot 7980400, Israel

* Correspondence: ayelet.harari@sheba.health.gov.il; Tel.: +972-3-5302006

† These authors contributed equally to this work.



Citation: Melnikov, N.; Kamari, Y.; Kandel-Kfir, M.; Barshack, I.; Ben-Amotz, A.; Harats, D.; Shaish, A.; Harari, A. β -Carotene from the Alga *Dunaliella bardawil* Decreases Gene Expression of Adipose Tissue Macrophage Recruitment Markers and Plasma Lipid Concentrations in Mice Fed a High-Fat Diet. *Mar. Drugs* **2022**, *20*, 433. <https://doi.org/10.3390/md20070433>

Academic Editors: Ki Hyun Kim, Mostafa Rateb and Hossam Hassan

Received: 6 April 2022

Accepted: 24 June 2022

Published: 29 June 2022

Publisher's Note: MDPI stays neutral with regard to jurisdictional claims in published maps and institutional affiliations.



Copyright: © 2022 by the authors. Licensee MDPI, Basel, Switzerland. This article is an open access article distributed under the terms and conditions of the Creative Commons Attribution (CC BY) license (<https://creativecommons.org/licenses/by/4.0/>).

Abstract: Vitamin A and provitamin A carotenoids are involved in the regulation of adipose tissue metabolism and inflammation. We examined the effect of dietary supplementation using all-trans and 9-cis β -carotene-rich *Dunaliella bardawil* alga as the sole source of vitamin A on obesity-associated comorbidities and adipose tissue dysfunction in a diet-induced obesity mouse model. Three-week-old male mice (C57BL/6) were randomly allocated into two groups and fed a high-fat, vitamin A-deficient diet supplemented with either vitamin A (HFD) or β -carotene (BC) (HFD-BC). Vitamin A levels in the liver, WATs, and BAT of the HFD-BC group were 1.5–2.4-fold higher than of the HFD group. BC concentrations were 5–6-fold greater in BAT compared to WAT in the HFD-BC group. The eWAT mRNA levels of the *Mcp-1* and *Cd68* were 1.6- and 2.1-fold lower, respectively, and the plasma cholesterol and triglyceride concentrations were 30% and 28% lower in the HFD-BC group compared with the HFD group. Dietary BC can be the exclusive vitamin A source in mice fed a high-fat diet, as shown by the vitamin A concentration in the plasma and tissues. Feeding BC rather than vitamin A reduces adipose tissue macrophage recruitment markers and plasma lipid concentrations.

Keywords: vitamin A; β -carotene; obesity; adipose tissue; mice

1. Introduction

Obesity is characterized by the excessive accumulation of fat in adipose tissue, which may impair health. Obesity is a major risk factor for cardiovascular diseases, type 2 diabetes, nonalcoholic fatty liver disease, and several types of cancers [1]. Although obesity has been recognized as a worldwide epidemic, the current interventions and treatments have many limitations. Several human studies have found correlations between obesity and low levels of serum or subcutaneous fat carotenoids [2–7].

Carotenoids are fat-soluble pigments synthesized in plants, fungi, bacteria, and algae. Provitamin A carotenoids, such as β -carotene (BC) and α -carotene, are cleaved in the body to produce vitamin A [8]. Vitamin A is an essential micronutrient for growth and development, vision, reproduction, and immunity in mammals. The main dietary sources of preformed vitamin A include meat and dairy products, while BC from plants serves as the primary provitamin A carotenoid in the human diet [8]. Vitamin A and provitamin A carotenoids are stored in the liver and adipose tissue. In these tissues, vitamin A and

provitamin A carotenoids can be converted into the biologically active derivatives of vitamin A: retinol, retinal, and retinoic acid (RA) [9,10]. Although the distribution of vitamin A in different rodent adipose depots has been examined [11,12], to the best of our knowledge, the accumulation of provitamin A carotenoids in rodent WAT and BAT has not been investigated.

In previous studies, we used the alga *Dunaliella bardawil* as a source for natural BC. This unicellular alga accumulates high BC concentrations (~10% of the dry weight), and it consists of two primary BC isomers: ~50% ATBC and ~50% 9-cis BC [13]. We have shown that dietary supplementation with 9-cis BC or a mixture of all-trans and 9-cis BC from *Dunaliella bardawil* can protect against atherogenesis and reduce plasma cholesterol concentrations in a mouse model of atherogenesis, while synthetic all-trans BC had the opposite effect [14]. In vitro and in vivo experiments have demonstrated that ATBC is enzymatically converted to all-trans RA (ATRA), while 9-cis BC is converted to both ATRA and 9-cis RA [15,16]. Both RA isomers are involved in the regulation of gene expression through the activation of nuclear receptors. Our studies have indicated that dietary *Dunaliella bardawil* supplementation may inhibit the development of obesity-associated pathological disorders, such as dyslipidemia, adipose tissue inflammation, diabetes, atherosclerosis, and fatty liver in *Ldlr*^{-/-}, *ApoE*^{-/-}, and *db/db* mice models [14,17–19]. These mouse models develop fatty liver when fed a high-fat diet [20–22]. Interestingly, another group recently reported that dietary BC, as an exclusive source of vitamin A, reduced plasma cholesterol concentration and atherosclerotic lesion size only when the production of vitamin A by enzymatic cleavage of BC is available [23,24]. This supports our hypothesis that the positive impact of *Dunaliella bardawil* supplementation in mice might be the result of the conversion of algal BC isomers into vitamin A derivatives.

So far, the effect of dietary BC supplementation on adiposity and adipose tissue metabolism has been investigated by relatively few studies utilizing non-obese animal models fed a standard diet containing vitamin A [25–27]. Moreover, the isomer composition of the BC used in these experiments has not been unspecified. Thus, it is likely that ATBC was the dominant isomer. In the current study, we sought to investigate the impact of dietary supplementation with ATBC and 9-cis BC-rich *Dunaliella bardawil* as the sole source of vitamin A on risk factors associated with obesity in a diet-induced obesity.

2. Results

2.1. Body Weight, Energy Intake, and Tissue Mass

Body weight was measured throughout the 23-week experiment. The rate of body weight gain was higher in the HFD-BC group than in the HFD control group between weeks 7 and 9 (Figure 1A). However, no differences between the groups were observed in either NMR body composition analysis after 14 weeks (Supplemental Figure S1) or body weight gain from the 10th week and onwards. At week 23, the WAT mass was 10% greater in the HFD-BC group than in the HFD group ($p < 0.05$). In contrast, the liver mass was similar (Figure 1C). Although we found a 5% increase in food intake in the HFD-BC group compared with the HFD group, this result could not be statistically analyzed because intake was measured per cage.

2.2. Tissue and Plasma Vitamin A Levels

Vitamin A levels (all-trans retinol) in the HFD-BC group were significantly higher in the liver, eWAT, iWAT, and iBAT, but not in the plasma, when compared with the HFD group (Table 1). As expected, vitamin A concentration in the liver, which is the primary vitamin A reservoir, was substantially higher than all adipose depots by two orders of magnitude ($p < 0.0001$) in both the HFD and HFD-BC groups. Within each group, vitamin A concentrations did not differ between eWAT, iWAT, and iBAT ($p > 0.99$).

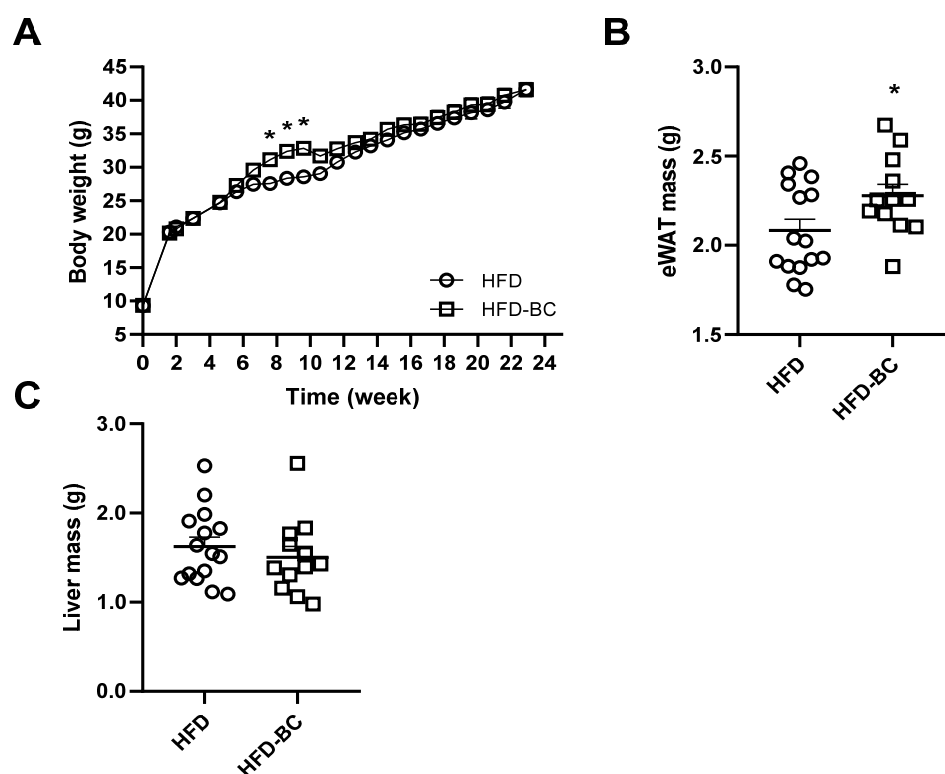


Figure 1. Three-week-old male mice were fed an HFD ($n = 15$) or an HFD-BC ($n = 13$) for 23 weeks. (A) Body weight throughout the experiment. (B) eWAT mass. (C) Liver mass. Values are means \pm SEM. * Different from HFD group, $p < 0.05$. BW, body weight; eWAT, epididymal white adipose tissue; HFD, high-fat diet; HFD-BC, high-fat diet supplemented with *Dunaliella bardawil*.

Table 1. Tissue and plasma retinol levels in mice fed an HFD or an HFD-BC for 23 weeks¹.

	HFD ($n = 5$)	HFD-BC ($n = 5$)
Liver retinol, $\mu\text{g/g}$ tissue	126 ± 15.8	194 ± 15.8 *
eWAT retinol, $\mu\text{g/g}$ tissue	0.21 ± 0.04	0.37 ± 0.03 *
iWAT retinol, $\mu\text{g/g}$ tissue	0.21 ± 0.01	0.50 ± 0.07 *
iBAT retinol, $\mu\text{g/g}$ tissue	0.25 ± 0.04	0.41 ± 0.03 *
Plasma retinol, $\mu\text{g/mL}$	0.19 ± 0.01	0.16 ± 0.03

¹ Data are presented as mean \pm SEM. * Different from HFD group, $p < 0.05$. iBAT, interscapular brown adipose tissue; iWAT, inguinal white adipose tissue.

2.3. Tissue and Plasma BC Concentrations

As expected, no isomers of BC were detected in the tissues of the mice in the HFD group supplemented exclusively with preformed vitamin A. On the other hand, both ATBC and 9-cis BC were detected in all analyzed samples of the HFD-BC group supplemented with BC given as *Dunaliella bardawil* powder (Table 2 and Figure 2). In the HFD-BC group, the plasma BC concentration was 0.48 ± 0.08 $\mu\text{g/mL}$, and the ATBC/9-cis BC ratio was 8.90 ± 1.45 ($n = 5$). Expectedly, the accumulation of total BC ($\mu\text{g/g}$ tissue) in the liver (7.04 ± 1.45) of the HFD-BC group was 20-fold, 17-fold, and 3-fold greater than eWAT, iWAT, and iBAT, respectively ($p < 0.001$). ATBC/9-cis BC ratio in the liver (1.82 ± 0.19) was lower by 3.7-fold, 2.7-fold, and 5.8-fold than in eWAT, iWAT, and iBAT, respectively, here suggesting that the liver stores more 9-cis BC than the adipose tissue ($p < 0.05$). The ATBC:9-cis BC isomer ratio in *Dunaliella bardawil* powder was about 1:1. Nevertheless, ATBC was the dominant isomer present in the plasma and tissues. Liver BC/retinol ratio (0.04 ± 0) was lower by 23-fold, 22-fold, and 130-fold than in eWAT, iWAT, and iBAT, respectively ($p < 0.05$). Surprisingly, iBAT BC concentration was elevated by 5–6-fold compared to eWAT and iWAT. As a result, the ratio between BC to retinol was higher in iBAT than in eWAT

and iWAT (Table 2). Furthermore, we found that the ATBC/9-cis BC ratio was elevated by 1.6- and 2.2-fold in iBAT compared with eWAT and iWAT, respectively (Table 2).

Table 2. Adipose tissue β -carotene levels, isomer ratios, and β -carotene/retinol ratios in mice fed an HFD-BC for 23 weeks ¹.

	eWAT (n = 5)	iWAT (n = 5)	iBAT (n = 5)
Total BC, $\mu\text{g/g}$ tissue ²	0.34 \pm 0.05b	0.41 \pm 0.04b	2.13 \pm 0.17a
ATBC/9-cis BC ratio	6.67 \pm 1.19b	4.91 \pm 0.54b	10.6 \pm 0.61a
BC/retinol ratio ²	0.95 \pm 0.15b	0.86 \pm 0.10b	5.20 \pm 0.46a

¹ Adipose tissue BC levels were measured by HPLC analysis. ² Total BC is the sum of ATBC and 9-cis BC concentrations. Data are presented as means \pm SEM. Labeled means in a row without a common letter differ, $p < 0.05$. ATBC, all-trans β -carotene; BC, β -carotene.

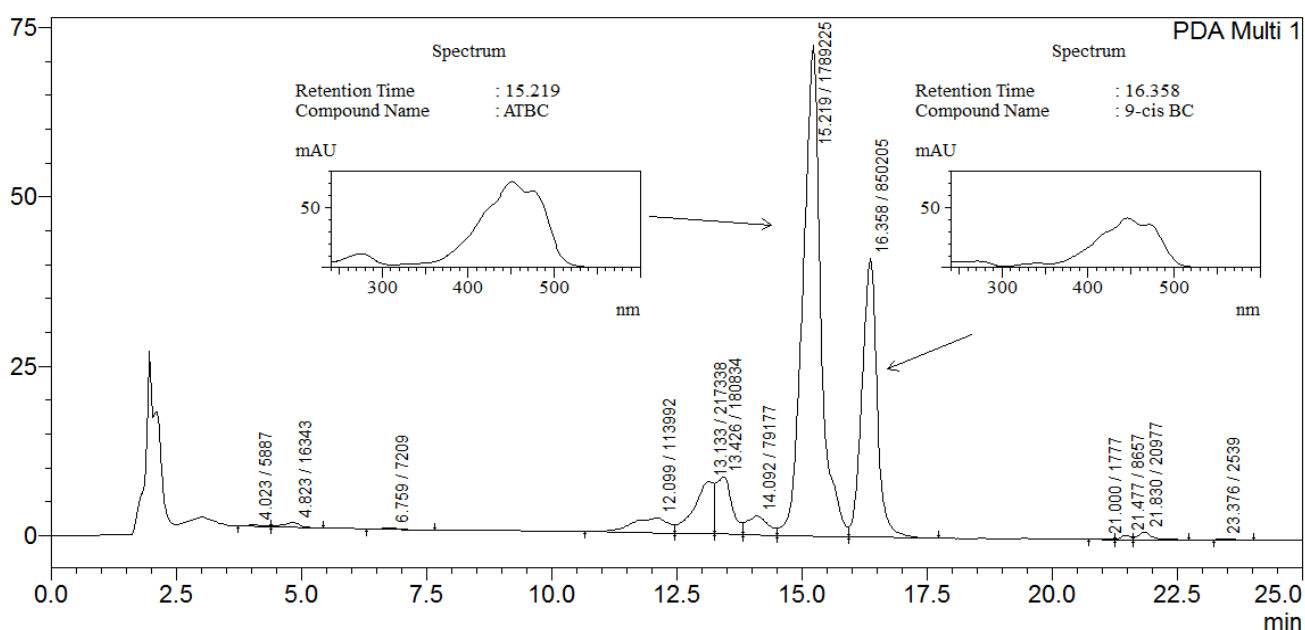


Figure 2. Representative HPLC analysis of hepatic carotenoids (spectrum range 200–700 AU) in a liver of a mouse in the HFD-BC group.

2.4. mRNA Levels of Inflammatory Cytokines and Transcriptional Regulators of Thermogenesis and Macrophage-Staining in Adipose Tissue

We examined the mRNA expression levels of inflammatory markers in eWAT and iBAT. The eWAT mRNA levels of *Mcp-1* and *Cd68*, which are markers for monocyte recruitment and tissue macrophages, were lower by 1.6- and 2.1-fold, respectively, in the HFD-BC group compared with the HFD group (Figure 3A). The mRNA levels of *Tnf α* and *Il-6* in eWAT and iBAT, as well as *Il-1 β* in eWAT, were not different between the diet groups (Figure 3A,B).

We also assessed eWAT and iBAT mRNA levels of *Ucp1*, which is expressed in thermogenically active adipocytes, and of the transcriptional regulators of *Ucp1*: *Ppar γ* and *Pgc1 α* [28]. No differences were found between the mRNA levels of *Pgc1 α* in iBAT or levels of *Ucp1* and *Ppar γ* in both eWAT and iBAT between the HFD-BC and HFD groups (Figure 3B).

In immunohistochemical staining of adipose tissue, we detected macrophage infiltration in adipose tissue of high-fat fed mice, while in *Dunaliella*-treated mice no macrophages were identified. (Figure 3C,D).

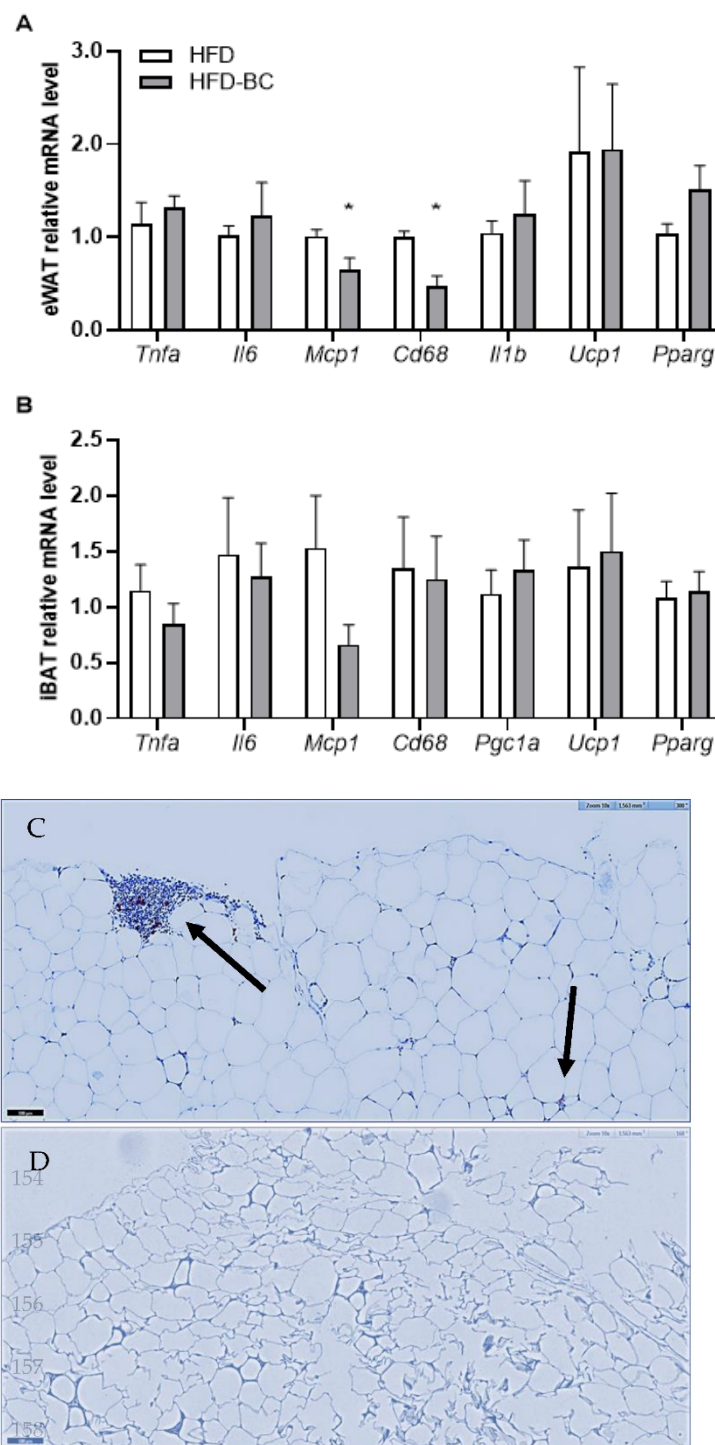


Figure 3. eWAT (**A**) and iBAT (**B**) relative mRNA levels ($n = 5-7$). Gapdh was used as a reference gene after 23 weeks. Histochemical detection of macrophages in epididymal adipose tissue of HFD (**C**) and HFD-BC (**D**); the bar = 100 micrometer. Black arrows indicate macrophages. Values are mean \pm SEM. * Different from HFD group, $p < 0.05$.

2.5. Plasma Lipids, Leptin, and Adiponectin Concentration

The plasma cholesterol and triglyceride levels in the HFD-BC group were decreased by 28% and 30%, respectively, compared with the HFD group after 23 weeks of treatment (Figure 4A,B). On the other hand, no differences were observed in the plasma leptin and adiponectin concentrations between the HFD-BC and HFD groups (Figure 4C,D).

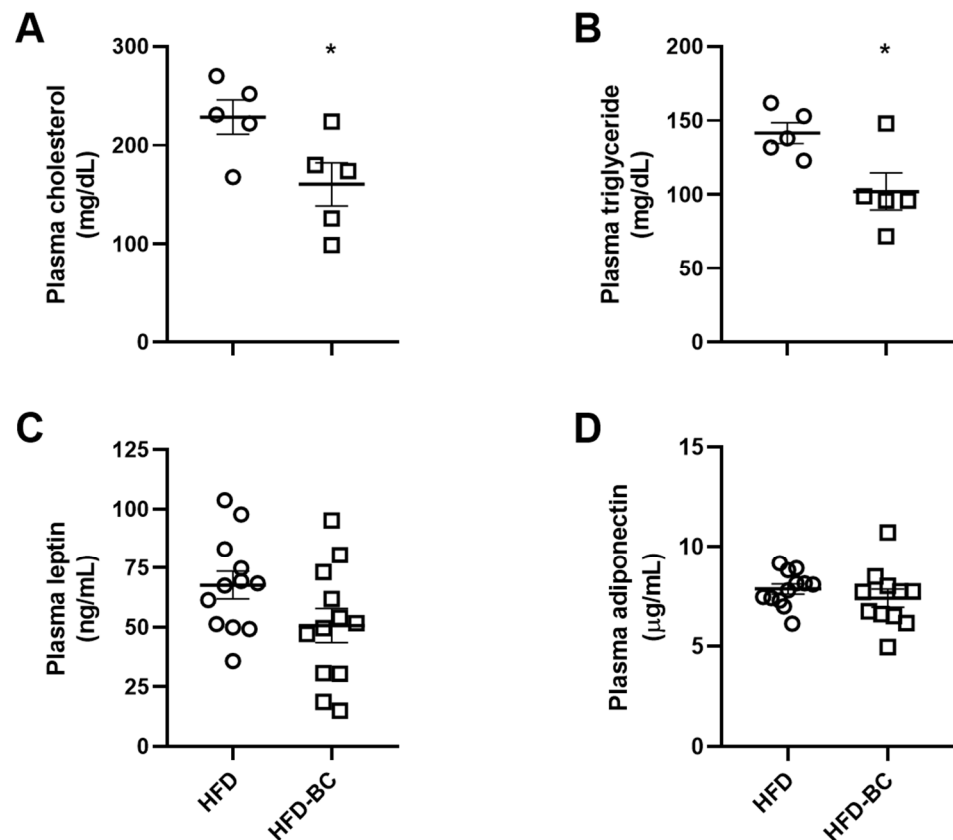


Figure 4. Fasting cholesterol (A), triglycerides (B), leptin (C), and adiponectin (D) concentrations in the plasma after 23 wk of treatment (A–B $n = 5$, C–D $n = 11$ –12). Values are mean \pm SEM. * Different from HFD group, $p < 0.05$.

2.6. Glucose Metabolism, White Adipocyte Size, and NAFLD

No significant differences were identified between the HFD-BC and HFD groups for all the following parameters: glucose tolerance (IPGTT), fasting blood glucose levels, fasting plasma insulin concentrations, the white adipocytes area in eWAT, and NAFLD activity score (Supplemental Figures S2–S4).

3. Discussion

In the current study, we investigated the effect of BC-rich *Dunaliella bardawil* powder as the sole source of vitamin A on the development of obesity and its complications in mice. We have demonstrated that dietary BC maintains tissue and plasma vitamin A reservoir and that BC accumulation in BAT was elevated compared with WAT. Unexpectedly, we found that BC supplementation increased eWAT mass but reduced eWAT mRNA levels of macrophage recruitment markers and lowered plasma cholesterol and triglyceride levels in high-fat diet fed mice. Contrary to our hypothesis, BC treatment did not affect the mRNA levels of the genes involved in regulating adipose tissue thermogenic activity in iBAT or eWAT.

Our previous study [29] showed that BC supplementation decreased atherogenesis in an *ApoE*^{−/−} mouse model compared with a vitamin A deficient group. In that study, both groups were fed a chow diet. Since ApoE can affect lipid metabolism, it is crucial to study BC in a wild-type model. Therefore, in the current study, we investigated the effect of BC in C57BL/6 mice fed a high-fat diet compared with the vitamin A-fed group. The present study demonstrates that dietary BC maintains vitamin A levels (all-trans retinol) in the liver, adipose tissue, and plasma. Although vitamin A levels in the tissues of the HFD-BC group were elevated compared with the controls, it is important to note that we did not adjust the relative quantity of vitamin A (retinol equivalent) in the HFD BC group to the

HFD control group. To the best of our knowledge, the estimated efficiency of BC isomer conversion to vitamin A in mice has not been evaluated [30]. Thus, adjusting the relative vitamin A content in the diets was not feasible. These results provide further evidence supporting BC's ability to maintain tissue and plasma vitamin A levels as an exclusive dietary source in mice.

In addition to vitamin A, we examined the accumulation of BC in mouse liver and adipose tissue. Here, we show that higher levels of BC accumulated in mouse BAT compared with WAT. To the best of our knowledge, the accumulation of BC in mouse BAT has not been studied, and we are the first to report this finding. Since BC storage in mouse tissues occurs only upon exposure to remarkably high dietary concentrations, BC is usually undetected in the tissues of mice fed standard diets that contain low levels of BC [31]. Thus, mice lacking the BC degradation enzyme β -Carotene oxygenase 1 (*Bco1*) are typically utilized to examine BC accumulation in tissues. However, it is impossible to study the role of BC as a provitamin A carotenoid in this model. By fortifying the high-fat diet to wild-type mice, we were able to study whether the presence of BC in adipose tissue together with vitamin A confers beneficial effects over the presence of vitamin A alone. With a high dose of BC, we detected ATBC and 9-cis BC in several tissues, studying the effect of BC as a sole source of vitamin A on obesity development in mice. As expected, BC accumulation in the liver, which is the primary reservoir of vitamin A and BC in mammals, was higher than in adipose tissue. Nevertheless, the ratio between BC and vitamin A concentrations in adipose tissue was greater compared with the liver ratio, suggesting that BC metabolism is distinct in each tissue. Taken together, our results imply that BC metabolism in mice differs between the liver and adipose tissue and between BAT and WAT.

Next, we investigated the effect of BC enrichment on body weight and adiposity. Unexpectedly, we discovered that eWAT mass was higher in the HFD BC group compared with the HFD control group. However, we found no differences in adipocyte hypertrophy or body weight gain during the second half of the experiment. Conversely, a previous study showed that BC supplementation decreased the masses of the three WAT depots examined: inguinal, gonadal, and retroperitoneal [27]. Nevertheless, the study was performed on female mice (C57BL/6) fed a standard diet. Further studies may be required to determine whether the effect of dietary BC supplementation on WAT mass in mice is influenced by diet composition and gender.

Furthermore, we examined the inflammatory state in eWAT by analyzing the mRNA levels of inflammatory-related genes. The mRNA levels of *Mcp-1* and *Cd68* in eWAT were significantly lower ($p < 0.05$) in the HFD-BC group compared with the HFD control group. Moreover, macrophages were detected in adipose tissue of HFD-treated mice, while no macrophages were found in *Dunaliella*-treated mice. Similarly, in a previous study, we demonstrated that BC dietary supplementation reduced the mRNA level of *Mcp-1* in the mesenteric WAT of obese *db/db* mice [17]. The *Mcp-1* levels in adipose tissue and plasma of obese rodents are increased and promote adipose tissue macrophage infiltration [32–34]. Additionally, a study in humans demonstrated that the mRNA levels of *Mcp-1* and *Cd68* (macrophage marker) were elevated in subcutaneous WAT of obese individuals [35]. Notably, BC treatment decreased the expression of *Mcp-1* and the activity of *NFkB*, which regulates the expression of proinflammatory cytokines, in cultured adipocytes exposed to oxidative stress [36]. In addition to BC, its downstream cleavage product ATRA has been shown to have an anti-inflammatory effect [37]. Altogether, these results suggest that a BC-rich diet may reduce adipose tissue macrophage recruitment, possibly because of the presence of vitamin A, BC, or both.

Moreover, we sought to assess measures of obesity-associated hyperlipidemia. The plasma concentrations of cholesterol and triglycerides were lower in the HFD-BC group compared with the HFD control group. In previous studies, we have demonstrated that BC (given as *Dunaliella bardawil*) decreased plasma cholesterol concentrations in atherosclerosis mouse models (*Apoe*^{-/-} and *Ldlr*^{-/-}), as well as triglyceride levels in obese diabetic (*db/db*) mice [14,17–19]. Of note, oxidized (BC-free) *Dunaliella bardawil* powder did not reduce

the plasma cholesterol concentration of *Ldlr*^{-/-} mice [14]. A recent study has shown that BC, when given as the sole source of vitamin A, decreased plasma cholesterol levels in wild-type mice but not in *Bco1*^{-/-} mice [23]. A follow-up study found that atherosclerotic lesion size and plasma cholesterol level were reduced by BC supplementation in *Ldlr*^{-/-} mice but not in *Ldlr*^{-/-}/*Bco1*^{-/-} mice [24]. Overall, these observations suggest that the effect of BC on plasma lipids is probably mediated by *Bco1*-dependent cleavage of BC to form RA, a derivative of vitamin A that binds to and activates the nuclear receptors involved in regulating metabolic pathways [23,24].

Finally, we evaluated the thermogenic activity in eWAT and BAT by gene expression analysis. BC, when given as the only dietary source of vitamin A, did not affect the mRNA levels of genes involved in regulating thermogenesis (*Ucp1*, *Pparγ*, and *Pgc1α*) in the eWAT or BAT of the HFD-BC group compared with the HFD group. To the best of our knowledge, the effect of BC supplementation on the expression of *Ucp1*, which plays a major role in brown and beige adipocyte thermogenic activity, has only been examined in vitro [38,39] and in standard-diet-fed ferrets [26]. Remarkably, a review of several studies has concluded that high-fat diets may increase the expression of *Ucp1* in rodent BAT, likely reflecting an adaptive mechanism to excess caloric intake [40]. Hence, it is conceivable that high-fat diet feeding might have masked a feasible effect of BC on adipose tissue thermogenic capacity.

The positive effects of BC can be attributed to its role as a precursor of retinol, RA, and other retinoids. However, additional research is required to elucidate whether BC itself could act directly in this manner. It was shown by Lobo et al. that retinoid signaling and the expression of *Pparγ* in the WAT of vitamin A-deficient mice were both affected by BC treatment, while all-trans-retinol had no effect [41]. In addition, the study showed that in mature adipocytes, BC, not all-trans-retinol was metabolized to RA. Furthermore, we recently showed that serum and adipose tissue carotenoids, including BC, but not retinol, negatively correlated to many anthropometric and metabolic traits in humans [2].

The current study implies that BC metabolism in mouse WAT and BAT is different. Still, possible molecular pathways that may explain this difference have not been investigated. Moreover, we show that supplementing high-fat diet-fed obese mice with ATBC and 9-cis BC, as an exclusive vitamin A source, decreases eWAT macrophage infiltration markers and reduces cholesterol and triglyceride plasma levels.

4. Materials and Methods

4.1. Mice

Three-week-old male mice (C57BL/6J^{OlaHsd}) were housed in plastic cages on wood-shaving bedding, under controlled ambient temperatures (23 ± 2 °C) and on a 12 h light/12 h dark cycle. The animals had free access to feed and water. The mice were killed after 23 weeks using isoflurane following a 15 h fast. Venous blood, liver, epididymal WAT (eWAT), inguinal WAT (iWAT), and interscapular BAT (iBAT) were collected. Blood samples were immediately centrifuged (10 min at 4 °C and 955 g), and the plasma was stored at -80 °C. Tissue samples were immediately snap-frozen in liquid nitrogen and stored at 80 °C until use. All procedures were performed in accordance with the Chaim Sheba Medical Center's Guidelines for Animal Studies and approved by the Institutional Animal Ethics Committee (ethical approval code 1204/19).

4.2. Diet

We used a vitamin A-deficient, high-fat diet (20% of the calories from protein, 20% from carbohydrate, 60% from fat, D06040702, Research Diets, Inc., New Brunswick, NJ, USA) fortified with either vitamin A as retinyl acetate (Sigma-Aldrich, St. Louis, MO, USA) or *Dunaliella bardawil* powder (Nikken Sohonsa, Gifu, Japan) containing ~10% of the dry weight as BC [13]. Detailed diet formulation is listed in Supplemental Table S1. To prepare the feed, 250 mL warm distilled water was mixed with 12 g fish gelatin until the solution became clear. Then, the gelatin solution was thoroughly mixed with 1 kg of feed and 4.5 mg of vitamin A (dissolved in 40 µL olive oil) or 80 g *Dunaliella bardawil* powder. The feed

mixtures were poured into containers and stored at $-20\text{ }^{\circ}\text{C}$. Since BC isomers are oxidized upon exposure to air and light, the BC content and ATBC/9-cis ratio in *Dunaliella bardawil* powder were examined before adding the alga to the feed. The feed was replaced every 2 days.

4.3. Study Design

The mice were allocated into two groups, 15 animals per group, while ensuring that the initial body weight variation was similar in each group. In each diet group, the mice were housed in two separate cages (6–8 animals per cage). The mice were fed for 23 weeks with either one of two high-fat diets: I. HFD, containing 4.5 mg vitamin A per kg feed, or II. HFD-BC containing 6–8 g BC (~50% all-trans and ~50% 9-cis) per kg feed. At the most, body weight and feed intake were recorded every 10 and 4 days, respectively. Body composition was determined in anaesthetized mice at the 14th week using a TD-NMRLF50 minispec Live Mice Analyzer (Bruker Optics, Billerica, MA, USA). The NMR instrument was calibrated according to the manufacturer's instructions, and the mice were weighed and inserted into the test chamber.

4.4. Carotenoid and Retinol Analysis

All-trans retinol (vitamin A) and BC isomer levels in plasma, liver ($n = 5$), and adipose tissue ($n = 5$) were determined by HPLC, as previously described by Harari et al. [29].

4.5. Analysis of Gene Expression by Real-Time PCR

An RNeasy Lipid Tissue Mini Kit (QIAGEN, Hilden, Germany) was used to extract RNA from eWAT ($n = 5$ –6) and iBAT ($n = 5$ –7). The extracted RNA quantity and quality were determined using NanoDrop One (Thermo Scientific, Wilmington, DE, USA), and the RNA was stored at $-80\text{ }^{\circ}\text{C}$. Equivalent amounts of the total RNA were reversely transcribed to cDNA using the High-Capacity cDNA Reverse Transcription Kit (Applied Biosystems, Waltham, MA, USA). Quantitative real-time PCR was performed in duplicates with the 7500 Real-Time PCR (Applied Biosystems, Waltham, MA, USA), FastStart Universal Probe Master ROX (Roche, Pleasanton, CA, USA), probes labeled at the 5' end with fluorescein (FAM) and at the 3' end with a dark quencher dye (Universal ProbeLibrary, Roche, Indianapolis, IN, USA) and custom primers (Sigma-Aldrich, St. Louis, MO, USA). A pre-designed qPCR assay (PrimeTime[®] Mini 135qPCR Assay, Integrated DNA Technologies, Coralville, IA, USA) was used for the quantification of *Ppar γ* expression. All probes and primers are listed in the Supplementary Data (Supplemental Table S2). Relative quantification was done using the $2^{-\Delta\Delta\text{CT}}$ method against control glyceraldehyde-3-phosphate dehydrogenase (*Gapdh*) [42]. The results are expressed as fold-change relative to the HFD group.

4.6. Adipose Tissue and Liver Histological Analysis

eWAT and liver samples were fixed in 4% formaldehyde buffered solution for 72 h and embedded in paraffin. Tissue sections (5 μm) were stained with hematoxylin and eosin (H&E) and visualized under a microscope at $20\times$ (Olym-144pus BX51 microscope, Olympus UPLanApo $20\times/0.70$ objective, Nikon DS-Fi1 camera, Olympus, Tokyo, Japan). Initial processing of the eWAT image sections was performed using AdipoCount software [43]. Then, the sizes and numbers of the adipocytes were measured using Fiji software [44] with Adiposoft plugin [45] in manual editing mode. Blinded scoring of the liver sections was performed by the Head of the Institute of Pathology at Sheba Medical Center (Prof. Iris Barshack), according to NAFLD activity score criteria [46,47]. Macrophage infiltration in adipose tissue was estimated by CD68 staining [48].

4.7. Analysis of Plasma Parameters

During the 18th week, retro-orbital blood samples were collected after a 4 h fast into collection tubes containing EDTA for insulin measurement, whereas terminal blood

samples (23rd week) were used to test all other parameters. We used a colorimetric enzymatic procedure to measure the total plasma cholesterol and triglycerides (AU480 chemistry analyzer, Beckman Coulter, Inc, Brea, CA, USA). Plasma insulin (MRC-10-1249-01, Mercodia, Uppsala, Sweden), leptin (MOB00, R&D Systems, Inc., Minneapolis, MN, USA), and adiponectin (MRP300, R&D Systems, Inc., Minneapolis, MN, USA) levels were measured using commercial ELISA following the manufacturer's protocols.

4.8. Intraperitoneal Glucose Tolerance Test and Fasting Glucose

An intraperitoneal glucose tolerance test (IPGTT) was performed during the 16th week of treatment by injecting weight-adjusted volumes of 20% (*w/v*) glucose solution (2 g glucose/kg body weight) after 4 h of fasting. IPGTT blood samples were measured at 0, 15, 30, 60, and 120 min. Fasting blood glucose (4 h) was assessed during the 18th week. All blood samples were collected from the tail vein, and glucose levels were measured using a glucometer (FreeStyle Lite, Abbott, Alameda, CA, USA).

4.9. Statistical Analyses

Data are expressed as the means \pm SEM. Statistical significance was defined as $p < 0.05$. Differences in body weight between the HFD and HFD-BC groups were analyzed by a mixed effects analysis, followed by Bonferroni's multiple comparisons test. Other differences between the two groups were analyzed by an unpaired Student's *t*-test or Mann-Whitney test (NAFLD activity score data). BC concentrations in tissues (WATs, BAT, liver) of the HFD-BC group were tested by 1-factor ANOVA followed by Tukey's multiple comparisons test, or by a Brown-Forsythe ANOVA followed by Tamhane's T2 multiple comparisons test. Statistical analysis and figures were generated using GraphPad Prism 8.

Supplementary Materials: The following supporting information can be downloaded at: <https://www.mdpi.com/article/10.3390/md20070433/s1>, Table S1: D06040702 Research Diets high-fat rodent diet formulation [49], Table S2: Real-Time PCR primers and probes (mouse). Figure S2: IPGTT (A) after 16 wk (4 h fast, $n = 7$). Blood glucose (B) and plasma insulin concentrations (C) after 18 wk (4 h fast, $n = 8$). Figure S3: eWAT adipocyte area (A) and liver NALFD activity score (B-E) after 23 weeks ($n = 4-5$). Figure S4: Representative images of eWAT (A) and liver (B) sections stained with H&E.

Author Contributions: Conceptualization, A.H., D.H. and A.S.; Methodology, N.M. and A.S.; Software, N.M.; Validation, A.H., M.K.-K. and A.S.; Formal Analysis, N.M. and I.B.; Investigation, N.M. and A.H.; Resources, D.H. and Y.K.; Data Curation, A.S. and A.H.; Writing—Original Draft Preparation, N.M.; Writing—Review & Editing, A.H., Y.K., A.S. and D.H.; Visualization, N.M. and A.B.-A.; Supervision, A.H., Y.K. and A.S.; Project Administration, N.M.; Funding Acquisition, D.H., A.S. and Y.K. All authors have read and agreed to the published version of the manuscript.

Funding: This research received no external funding.

Institutional Review Board Statement: The animal study protocol was approved by the Institutional Review Board (or Ethics Committee) of Sheba Medical Center (protocol code 1180/18, date of approval 10.4.2019, protocol code 1204/19 date of approval 16 June 2019).

Data Availability Statement: Not applicable.

Conflicts of Interest: A.S. and D.H. are supported by Nikken Sohonsha Corporation, Japan. The company had no role in the study design, data collection and analysis, decision to publish, or preparation of the manuscript. N.B.T. Israel provided support in the form of a salary for author A.B.A. but did not have any additional role in the study design, data collection and analysis, decision to publish, or preparation of the manuscript.

References

1. Hruby, A.; Hu, F.B. The Epidemiology of Obesity: A Big Picture. *Pharmacoeconomics* **2015**, *33*, 673–689. [[CrossRef](#)] [[PubMed](#)]
2. Harari, A.; Coster, A.C.; Jenkins, A.; Xu, A.; Greenfield, J.R.; Harats, D.; Shaish, A.; Samocho-Bonet, D. Obesity and Insulin Resistance Are Inversely Associated with Serum and Adipose Tissue Carotenoid Concentrations in Adults. *J. Nutr.* **2019**, *150*, 38–46. [[CrossRef](#)] [[PubMed](#)]
3. Neuhouser, M.L.; Rock, C.L.; Eldridge, A.L.; Kristal, A.R.; Patterson, R.E.; Cooper, D.A.; Neumark-Sztainer, D.; Cheskin, L.J.; Thornquist, M.D. Serum Concentrations of Retinol, α -Tocopherol and the Carotenoids Are Influenced by Diet, Race and Obesity in a Sample of Healthy Adolescents. *J. Nutr.* **2001**, *131*, 2184–2191. [[CrossRef](#)]
4. Burrows, T.L.; Warren, J.M.; Colyvas, K.; Garg, M.L.; Collins, C.E. Validation of overweight children's fruit and vegetable intake using plasma carotenoids. *Obesity* **2009**, *17*, 162–168. [[CrossRef](#)] [[PubMed](#)]
5. de Souza Valente da Silva, L.; Valeria da Veiga, G.; Ramalho, R.A. Association of serum concentrations of retinol and carotenoids with overweight in children and adolescents. *Nutrition* **2007**, *23*, 392–397. [[CrossRef](#)] [[PubMed](#)]
6. Wang, L.; Gaziano, J.M.; Norkus, E.P.; Buring, J.E.; Sesso, H.D. Associations of plasma carotenoids with risk factors and biomarkers related to cardiovascular disease in middle-aged and older women. *Am. J. Clin. Nutr.* **2008**, *88*, 747–754. [[CrossRef](#)]
7. Östh, M.; Öst, A.; Kjolhede, P.; Strålfors, P. The concentration of β -carotene in human adipocytes, but not the whole-body adipocyte stores, is reduced in obesity. *PLoS ONE* **2014**, *9*, e85610. [[CrossRef](#)]
8. Bonet, M.L.; Canas, J.A.; Ribot, J.; Palou, A. Carotenoids in Adipose Tissue Biology and Obesity. *Subcell. Biochem.* **2016**, *79*, 377–414. [[CrossRef](#)]
9. Tanumihardjo, S.A.; Russell, R.M.; Stephensen, C.B.; Gannon, B.M.; Craft, N.E.; Haskell, M.J.; Lietz, G.; Schulze, K.; Raiten, D.J. Biomarkers of Nutrition for Development (BOND)—Vitamin A Review. *J. Nutr.* **2016**, *1461*, 1816S–1848S. [[CrossRef](#)]
10. Bonet, M.L.; Canas, J.A.; Ribot, J.; Palou, A. Carotenoids and their conversion products in the control of adipocyte function, adiposity and obesity. *Arch. Biochem. Biophys.* **2015**, *572*, 112–125. [[CrossRef](#)]
11. Tsutsumi, C.; Okuno, M.; Tannous, L.; Piantedosi, R.; Allan, M.; Goodman, D.S.; Blaner, W.S. Retinoids and retinoid-binding protein expression in rat adipocytes. *J. Biol. Chem.* **1992**, *267*, 1805–1810. [[CrossRef](#)]
12. Kane, M.A.; Folias, A.E.; Napoli, J.L. HPLC/UV quantitation of retinal, retinol, and retinyl esters in serum and tissues. *Anal. Biochem.* **2008**, *378*, 71–79. [[CrossRef](#)] [[PubMed](#)]
13. Ben-Amotz, A.; Avron, M. On the Factors Which Determine Massive beta-Carotene Accumulation in the Halotolerant Alga *Dunaliella bardawil*. *Plant Physiol.* **1983**, *72*, 593–597. [[CrossRef](#)]
14. Harari, A.; Harats, D.; Marko, D.; Cohen, H.; Barshack, I.; Kamari, Y.; Gonen, A.; Gerber, Y.; Ben-Amotz, A.; Shaish, A. A 9-cis β -carotene-enriched diet inhibits atherogenesis and fatty liver formation in LDL receptor knockout mice. *J. Nutr.* **2008**, *138*, 1923–1930. [[CrossRef](#)] [[PubMed](#)]
15. Wang, X.D.; Krinsky, N.I.; Benotti, P.N.; Russell, R.M. Biosynthesis of 9-cis-retinoic acid from 9-cis-beta-carotene in human intestinal mucosa in vitro. *Arch. Biochem. Biophys.* **1994**, *313*, 150–155. [[CrossRef](#)] [[PubMed](#)]
16. Hébuterne, X.; Wang, X.D.; Johnson, E.J.; Krinsky, N.I.; Russell, R.M. Intestinal absorption and metabolism of 9-cis-beta-carotene in vivo: Biosynthesis of 9-cis-retinoic acid. *J. Lipid Res.* **1995**, *36*, 1264–1273. [[CrossRef](#)]
17. Harari, A.; Harats, D.; Marko, D.; Cohen, H.; Barshack, I.; Gonen, A.; Ben-Shushan, D.; Kamari, Y.; Ben-Amotz, A.; Shaish, A. Supplementation with 9-cis β -carotene-rich alga *Dunaliella* improves hyperglycemia and adipose tissue inflammation in diabetic mice. *J. Appl. Phycol.* **2013**, *25*, 687–693. [[CrossRef](#)]
18. Relevy, N.Z.; Rühl, R.; Harari, A.; Grosskopf, I.; Barshack, I. 9-cis β -carotene Inhibits Atherosclerosis Development in Female LDLR^{-/-} Mice. *Funct. Foods Health Dis.* **2015**, *5*, 67–79. [[CrossRef](#)]
19. Harari, A.; Abecassis, R.; Relevy, N.; Levi, Z.; Ben-Amotz, A.; Kamari, Y.; Harats, D.; Shaish, A. Prevention of atherosclerosis progression by 9-cis-beta-carotene rich alga *dunaliella* in apoE-deficient mice. *Biomed. Res. Int.* **2013**, *2013*, 169517. [[CrossRef](#)]
20. Santhekadur, P.K.; Kumar, D.P.; Sanyal, A.J. Preclinical models of non-alcoholic fatty liver disease. *J. Hepatol.* **2018**, *68*, 230–237. [[CrossRef](#)]
21. Bieghs, V.; Van Gorp, P.J.; Wouters, K.; Hendrikkx, T.; Gijbels, M.J.; van Bilsen, M.; Bakker, J.; Binder, C.J.; Lütjohann, D.; Staels, B.; et al. LDL Receptor Knock-Out Mice Are a Physiological Model Particularly Vulnerable to Study the Onset of Inflammation in Non-Alcoholic Fatty Liver Disease. *PLoS ONE* **2012**, *7*, e30668. [[CrossRef](#)] [[PubMed](#)]
22. Nasiri-Ansari, N.; Nikolopoulou, C.; Papoutsis, K.; Kyrou, I.; Mantzoros, C.S.; Kyriakopoulos, G.; Chatzigeorgiou, A.; Kalotychou, V.; Randeve, M.S.; Chatha, K.; et al. Empagliflozin Attenuates Non-Alcoholic Fatty Liver Disease (NAFLD) in High Fat Diet Fed ApoE^{-/-} Mice by Activating Autophagy and Reducing ER Stress and Apoptosis. *Int. J. Mol. Sci.* **2021**, *22*, 818. [[CrossRef](#)] [[PubMed](#)]
23. Amengual, J.; Coronel, J.; Marques, C.; Aradillas-García, C.; Morales, J.M.V.; Andrade, F.C.D.; Erdman, J.W.; Teran-Garcia, M. β -Carotene Oxygenase 1 Activity Modulates Circulating Cholesterol Concentrations in Mice and Humans. *J. Nutr.* **2020**, *150*, 2023–2030. [[CrossRef](#)] [[PubMed](#)]
24. Zhou, F.; Wu, X.; Pinos, I.; Abraham, B.M.; Barrett, T.J.; von Lintig, J.; Fisher, E.A.; Amengual, J. β -Carotene conversion to vitamin A delays atherosclerosis progression by decreasing hepatic lipid secretion in mice. *J. Lipid Res.* **2020**, *61*, 1491–1503. [[CrossRef](#)]
25. Murano, I.; Morroni, M.; Zingaretti, M.C.; Oliver, P.; Sánchez, J.; Fuster, A.; Picó, C.; Palou, A.; Cinti, S. Morphology of ferret subcutaneous adipose tissue after 6-month daily supplementation with oral beta-carotene. *Biochim. Biophys. Acta* **2005**, *1740*, 305–312. [[CrossRef](#)] [[PubMed](#)]

26. Sánchez, J.; Fuster, A.; Oliver, P.; Palou, A.; Picó, C. Effects of beta-carotene supplementation on adipose tissue thermogenic capacity in ferrets (*Mustela putorius furo*). *Br. J. Nutr.* **2009**, *102*, 1686–1694. [[CrossRef](#)]
27. Amengual, J.; Gouranton, E.; van Helden, Y.G.J.; Hessel, S.; Ribot, J.; Kramer, E.; Kiec-Wilk, B.; Razny, U.; Lietz, G.; Wyss, A.; et al. Beta-carotene reduces body adiposity of mice via BCMO1. *PLoS ONE* **2011**, *6*, e20644. [[CrossRef](#)]
28. Bonet, M.L.; Oliver, P.; Palou, A. Pharmacological and nutritional agents promoting browning of white adipose tissue. *Biochim. Biophys. Acta* **2013**, *1831*, 969–985. [[CrossRef](#)]
29. Harari, A.; Melnikov, N.; Kfir, M.K.; Kamari, Y.; Mahler, L.; Ben-amotz, A.; Harats, D.; Cohen, H.; Shaish, A. Dietary β -carotene rescues vitamin a deficiency and inhibits atherogenesis in apolipoprotein e-deficient mice. *Nutrients* **2020**, *12*, 1625. [[CrossRef](#)]
30. Green, A.S.; Fascetti, A.J. Meeting the Vitamin A Requirement: The Efficacy and Importance of β -Carotene in Animal Species. *Sci. World J.* **2016**, *2016*, 7393620. [[CrossRef](#)]
31. Coronel, J.; Pinos, I.; Amengual, J. β -carotene in Obesity Research: Technical Considerations and Current Status of the Field. *Nutrients* **2019**, *11*, 842. [[CrossRef](#)] [[PubMed](#)]
32. Kanda, H.; Tateya, S.; Tamori, Y.; Kotani, K.; Hiasa, K.; Kitazawa, R.; Kitazawa, S.; Miyachi, H.; Maeda, S.; Egashira, K.; et al. MCP-1 contributes to macrophage infiltration into adipose tissue, insulin resistance, and hepatic steatosis in obesity. *J. Clin. Invest.* **2006**, *116*, 1494–1505. [[CrossRef](#)] [[PubMed](#)]
33. Sartipy, P.; Loskutoff, D.J. Monocyte chemoattractant protein 1 in obesity and insulin resistance. *Proc. Natl. Acad. Sci. USA* **2003**, *100*, 7265–7270. [[CrossRef](#)]
34. Makki, K.; Froguel, P.; Wolowczuk, I. Adipose tissue in obesity-related inflammation and insulin resistance: Cells, cytokines, and chemokines. *ISRN Inflamm.* **2013**, *2013*, 139239. [[CrossRef](#)]
35. Fjeldborg, K.; Pedersen, S.B.; Møller, H.J.; Christiansen, T.; Bennetzen, M.; Richelsen, B. Human adipose tissue macrophages are enhanced but changed to an anti-inflammatory profile in obesity. *J. Immunol. Res.* **2014**, *2014*, 309548. [[CrossRef](#)]
36. Cho, S.O.; Kim, M.-H.; Kim, H. β -Carotene Inhibits Activation of NF- κ B, Activator Protein-1, and STAT3 and Regulates Abnormal Expression of Some Adipokines in 3T3-L1 Adipocytes. *J. Cancer Prev.* **2018**, *23*, 37–43. [[CrossRef](#)] [[PubMed](#)]
37. Karkeni, E.; Bonnet, L.; Astier, J.; Couturier, C.; Dalifard, J.; Tourniaire, F.; Landrier, J.F. All-trans-retinoic acid represses chemokine expression in adipocytes and adipose tissue by inhibiting NF- κ B signaling. *J. Nutr. Biochem.* **2017**, *42*, 101–107. [[CrossRef](#)] [[PubMed](#)]
38. Serra, F.; Bonet, M.L.; Puigserver, P.; Oliver, J.; Palou, A. Stimulation of uncoupling protein 1 expression in brown adipocytes by naturally occurring carotenoids. *Int. J. Obes. Relat. Metab. Disord.* **1999**, *23*, 650–655. [[CrossRef](#)] [[PubMed](#)]
39. Shabalina, I.G.; Backlund, E.C.; Bar-Tana, J.; Cannon, B.; Nedergaard, J. Within brown-fat cells, UCP1-mediated fatty acid-induced uncoupling is independent of fatty acid metabolism. *Biochim. Biophys. Acta Bioenerg.* **2008**, *1777*, 642–650. [[CrossRef](#)]
40. Fromme, T.; Klingenspor, M. Uncoupling protein 1 expression and high-fat diets. *Am. J. Physiol. Regul. Integr. Comp. Physiol.* **2011**, *300*, R1–R8. [[CrossRef](#)]
41. Lobo, G.P.; Amengual, J.; Li, H.N.M.; Golczak, M.; Bonet, M.L.; Palczewski, K.; von Lintig, J. Beta,beta-carotene decreases peroxisome proliferator receptor gamma activity and reduces lipid storage capacity of adipocytes in a beta,beta-carotene oxygenase 1-dependent manner. *J. Biol. Chem.* **2010**, *285*, 27891–27899. [[CrossRef](#)] [[PubMed](#)]
42. Livak, K.J.; Schmittgen, T.D. Analysis of relative gene expression data using real-time quantitative PCR and the 2- $\Delta\Delta$ CT method. *Methods* **2001**, *25*, 402–408. [[CrossRef](#)] [[PubMed](#)]
43. Zhi, X.; Wang, J.; Lu, P.; Jia, J.; Shen, H.B.; Ning, G. AdipoCount: A new software for automatic adipocyte counting. *Front. Physiol.* **2018**, *9*, 85. [[CrossRef](#)] [[PubMed](#)]
44. Schindelin, J.; Arganda-Carreras, I.; Frise, E.; Kaynig, V.; Longair, M.; Pietzsch, T.; Preibisch, S.; Rueden, C.; Saalfeld, S.; Schmid, B.; et al. Fiji: An open-source platform for biological-image analysis. *Nat. Methods* **2012**, *9*, 676–682. [[CrossRef](#)]
45. Galarraga, M.; Campi3n, J.; Mun3n-Barrutia, A.; Boqu3, N.; Moreno, H.; Mart3nez, J.A.; Milagro, F.; Ortiz-de-Sol3rzano, C. Adiposoftware: Automated software for the analysis of white adipose tissue cellularity in histological sections. *J. Lipid Res.* **2012**, *53*, 2791–2796. [[CrossRef](#)]
46. Kleiner, D.E.; Brunt, E.M.; Van Natta, M.; Behling, C.; Contos, M.J.; Cummings, O.W.; Ferrell, L.D.; Liu, Y.C.; Torbenson, M.S.; Unalp-Arida, A.; et al. Design and validation of a histological scoring system for nonalcoholic fatty liver disease. *Hepatology* **2005**, *41*, 1313–1321. [[CrossRef](#)]
47. Liang, W.; Menke, A.L.; Driessen, A.; Koek, G.H.; Lindeman, J.H.; Stoop, R.; Havekes, L.M.; Kleemann, R.; Van Den Hoek, A.M. Establishment of a general NAFLD scoring system for rodent models and comparison to human liver pathology. *PLoS ONE* **2014**, *9*, e115922. [[CrossRef](#)]
48. Lumeng, C.N.; Bodzin, J.L.; Saltiel, A.R. Obesity induces a phenotypic switch in adipose tissue macrophage polarization. *J. Clin. Invest.* **2007**, *117*, 175–184. [[CrossRef](#)]
49. Takemura, N.; Hagio, M.; Ishizuka, S.; Ito, H.; Morita, T.; Sonoyama, K. Inulin prolongs survival of intragastrically administered *Lactobacillus plantarum* no. 14 in the gut of mice fed a high-fat diet. *J. Nutr.* **2010**, *140*, 1963–1969. [[CrossRef](#)]